

Antiangiogenic Activity of the Endocannabinoid Anandamide: Correlation to its Tumor-Suppressor Efficacy

SIMONA PISANTI,¹ CRISTINA BORSELLI,² OLIMPIA OLIVIERO,² CHIARA LAEZZA,³ PATRIZIA GAZZERRO,¹ AND MAURIZIO BIFULCO^{1*}

¹Department of Pharmaceutical Sciences, University of Salerno, Fisciano, Salerno, Italy

²Department of Material and Production Engineering, University of Napoli "Federico II," Napoli, Italy

³IEOS, CNR, Napoli, Italy

Endocannabinoids are now emerging as suppressors of key cell-signaling pathways involved in cancer cell growth, invasion, and metastasis. We have previously observed that the metabolically stable anandamide analog, 2-methyl-2'-F-anandamide (Met-F-AEA) can inhibit the growth of thyroid cancer *in vivo*. Our hypothesis was that the anti-tumor effect observed could be at least in part ascribed to inhibition of neo-angiogenesis. Therefore, the aim of this study was to assess the anti-angiogenic activity of Met-F-AEA, to investigate the molecular mechanisms underlying this effect and whether Met-F-AEA could antagonize tumor-induced endothelial cell sprouting. We show that Met-F-AEA inhibited bFGF-stimulated endothelial cell proliferation, in a dose-dependent manner, and also induced apoptosis, both effects reliant on cannabinoid CB1 receptor stimulation. Analyzing the signaling pathways implicated in angiogenesis, we observed that the bFGF-induced ERK phosphorylation was antagonized by Met-F-AEA, and we found that p38 MAPK was involved in Met-F-AEA-induced apoptosis. Moreover, Met-F-AEA was able to inhibit bi-dimensional capillary-like tube formation and activity of matrix metalloprotease MMP-2, a major matrix degrading enzyme. Importantly, we demonstrated that Met-F-AEA is also functional *in vivo* since it inhibited angiogenesis in the chick chorioallantoic neovascularization model. Finally, Met-F-AEA inhibited tumor-induced angiogenesis in a three-dimensional model of endothelial and thyroid tumor cell (KiMol) spheroids co-cultures in different 3-D polymeric matrices that resemble tumor microenvironment and architecture. Thus, our results suggest that anandamide could be involved in the control of cancer growth targeting both tumor cell proliferation and the angiogenic stimulation of the vasculature.

J. Cell. Physiol. 211: 495–503, 2007. © 2006 Wiley-Liss, Inc.

Angiogenesis, the generation of new capillary blood vessels from the pre-existing vessels, is a complex process required in many physiological and pathological conditions (Risau, 1997). It is a main mechanism of vascularization during embryonic development, but in adult most blood vessels remain quiescent and neo-angiogenesis occurs, under tight regulation, only in the female reproductive system during cycling ovary, corpus luteum formation, in the placenta, and during wound healing and repair (Carmeliet, 2003). Unregulated angiogenesis is involved in different pathological processes, such as rheumatoid arthritis, diabetic retinopathy, psoriasis, tumor growth, and metastasis (Folkman, 1995). Complex and diverse cellular actions are implicated in angiogenesis, such as extracellular matrix degradation, proliferation and migration of endothelial cells, and morphological differentiation of endothelial cells to form tubes (Bussolino et al., 1997). The process requires a finely tuned balance between stimulatory and inhibitory signals such as growth factors, integrins, angiopoietins, chemokines, oxygen sensors, endogenous inhibitors, and many others (Carmeliet, 2003). Among these factors, vascular endothelial growth factor (VEGF), a soluble angiogenic factor produced by both normal and tumor cells, plays a key role in regulating normal and abnormal angiogenesis (Ferrara and Kerbel, 2005). The endogenous cannabinoid system, comprising the cannabinoid receptors CB1 and CB2, their endogenous ligands (endocannabinoids, e.g., anandamide), and the proteins that regulate endocannabinoid biosynthesis and degradation, controls several physiological and pathological conditions. The ubiquity of the endocannabinoids, and their modulating activity on proteins and nuclear factors involved in cell proliferation, differentiation, and apoptosis, suggests that the endocannabinoid signaling system is involved, among other

effects, in the control of cell survival and proliferation (De Petrocellis et al., 2004). Recent results suggest that the endocannabinoid system might provide a significant contribution to tumor growth and metastasis therapies (Bifulco and Di Marzo, 2002). In fact, endocannabinoids influence the intracellular events controlling the proliferation of numerous types of cancer cells, thereby leading to both *in vitro* and *in vivo* anti-tumor effects (Guzman, 2003; Bifulco et al., 2006). Increasing evidence suggests that anti-tumor effect of cannabinoid-related drugs could be at least in part ascribed to the inhibition of tumor neo-angiogenesis in animal models

Abbreviations: Met-F-AEA, 2-methyl-2'-F-anandamide; bFGF, basic fibroblast growth factor; ERK, extracellular-signal-regulated protein kinases; MAPK, mitogen activated protein kinases; VEGF, vascular endothelial growth factor; PAE, porcine aortic endothelial; HUVEC, human umbilical vein endothelial cells; CAM, chorioallantoic membrane assay; MMP, metalloproteases; PMA, phorbol myristate acetate; HA, hyaluronic acid; SIPNs, semi-interpenetrated networks; CLS, capillary-like sprouts; ECM, extracellular matrix.

Simona Pisanti and Cristina Borselli contributed equally to work.

*Correspondence to: Maurizio Bifulco, Dip. di Scienze Farmaceutiche, Università degli Studi di Salerno, 84084 Fisciano, Salerno, Italy. E-mail: maubiful@unisa.it; maubiful@unina.it

Received 13 September 2006; Accepted 25 October 2006

DOI: 10.1002/jcp.20954

(Portella et al., 2003). Recent studies have reported that the activation of CBI receptor inhibited angiogenesis via inhibition of VEGF expression, interference with endothelial cell migration and induction of endothelial cell apoptosis, thereby retarding skin cancer and glioma growth in vivo (Blazquez et al., 2003; Casanova et al., 2003). We previously showed that the downregulation of both VEGF and its receptor Flt-1, induced in vivo by anandamide, may lead to a direct effect on tumor neo-angiogenesis, growth, and metastasis (Portella et al., 2003). Nevertheless, the mechanism and the extent of endocannabinoids anti-angiogenic effects have not been fully explored to date.

In the present study, using porcine aortic endothelial cells (PAE) and human umbilical vein endothelial cells (HUVECs), we investigated the potential anti-angiogenic effect of a metabolically stable anandamide analog, 2-methyl-2'-F-anandamide (Met-F-AEA), in two-dimensional and three-dimensional angiogenic models in vitro and in the chick chorioallantoic membrane assay (CAM) in vivo. For three-dimensional assays, PAE and KiMol (rat thyroid v-K-ras transformed cells) tumor cell spheroids were co-cultured in different polymeric matrices, in order to better mimic the in vivo tumor microenvironment and architecture. Our data demonstrate that anandamide inhibits endothelial cell proliferation in vitro, angiogenesis in vivo, and also tumor-induced angiogenesis in 3D assays, suggesting its potential as an anti-angiogenic agent.

Materials and Methods

Drugs and antibodies

Met-F-AEA and p38 MAPK inhibitor SB203580 were purchased from Sigma (St. Louis, MO). The selective CBI antagonist, SR141716, was kindly provided by Sanofi-Synthelabo (Montpellier, France). Acid solution (pH 2) of pepsin-solubilized bovine dermal type I collagen (Vitrogen) was from Angiotech Biomaterials, Corp. (Palo Alto, CA). Rooster origin sodium-hyaluronan (Na-HA) was kindly provided by FAB (Fidia Advanced Biopolymers S.P.A., Abano Terme, Italy). The anti-CB1R and anti-pERK antibodies were purchased from Santa Cruz Biotechnology, Inc. (Santa Cruz, CA). The anti-I κ B and anti-plk β (Ser32) were from Cell Signaling (Danvers, MA). Matrigel was obtained from BD Biosciences (San Jose, CA).

The phosphorothioate oligonucleotides, corresponding to the *kB* consensus sequence (5'-CCTTGAAGGGATTTCCCTCC-3') or its mutated (scrambled) form (5'-CCTTGAATTTAAATCC-3') were purchased from Primm Srl (Milan, Italy) (Romano et al., 1998).

Cell lines and cell cultures

HUVECs were isolated from freshly delivered umbilical cords, as previously described (Hisano et al., 1999) and cultured in DMEM supplemented with 10% inactivated FBS and 2 mM L-glutamine. HUVECs at two to six passages were used in this study. Pig aortic endothelial (PAE) cells were kindly donated by Prof. F. Bussolino (IRCC, University of Turin, Turin, Italy). Kimol cells, derived from FRTL-5 cells on infection and transformation with wild-type strain of KiMSV-MoIMuLV, were kindly provided by Prof. G. Vecchio and A. Fusco. PAE cells and KiMol cells were cultured in Ham's F12 medium supplemented, respectively, with 10 or 5% inactivated FBS and 2 mM L-glutamine. Cells were cultured at 37°C in a humidified 5% CO₂ atmosphere. Cell culture reagents were all obtained from Gibco (Grand Island, NY).

Proliferation assay

The effects of Met-F-AEA on endothelial cell proliferation were evaluated, in vitro, by measuring [³H]thymidine incorporation. In brief, 3 × 10⁴ cells/ml were seeded into 96-well plates and immediately treated with the drugs in presence or not of bFGF (10 ng/ml), incubated for 24 h at 37°C (5% CO₂), then pulsed with 0.5 μCi/well of [³H]thymidine (Amersham Biosciences-GE Healthcare Europe, Milan, Italy) and harvested 4 h later. Radioactivity was measured in a scintillation counter (Wallac, Turku, Finland).

Assessment of apoptosis by annexin-V/propidium iodide double-staining assay

The cells were incubated for 24 h with Met-F-AEA, then collected, washed with PBS, and re-suspended at 1 × 10⁶ cells/ml in annexin V binding buffer (0.01 M HEPES, pH 7.4; 0.14 M NaCl; 2.5 mM CaCl₂). Apoptotic cell death was identified by double supra-vital staining with recombinant FITC-conjugated annexin-V-antibody (Dakocytomation) and propidium iodide. Flow cytometric analysis was performed immediately after staining. Data acquisition and analysis were performed in a Becton Dickinson FACSCalibur flow cytometer using CellQuest software. Each sample was analyzed using 10,000 events.

Cell-cycle analysis

Cells were collected, fixed in 300 μl of PBS plus 700 μl of ethanol 70%, and kept at -20°C o.n. Propidium iodide (10 μg/ml) in PBS containing 100 U/ml DNase-free RNase A was added to the cells; after 15 min at room temperature cells were subjected to flow cytometric analysis using ModFit LT v3.0 program from Verity Software House, Inc. (Topsham, ME). Each sample was analyzed using 10,000 events corrected for debris and aggregate populations.

Western blot analysis

Cells were plated in 100-mm dishes (Falcon, Becton-Dickinson Labware, Franklin Lakes, NJ) in regular medium with serum. After reaching sub-confluence, cells were starved for at least 6 h and then pre-incubated with Met-F-AEA for 30 min before stimulation with bFGF (Gibco) for 15 min. Cells were then washed with ice-cold phosphate-buffered saline and scraped into lysis buffer (50 mM Tris-HCl, 150 mM NaCl, 0.5% Triton X-100, 0.5% deossicollic acid, 10 mg/ml leupeptin, 2 mM phenylmethylsulfonyl fluoride, 10 mg/ml aprotinin). After removal of cell debris by centrifugation (14,500g, for 10 min at 4°C), protein was estimated. About 50 μg of proteins were loaded on 12% SDS-polyacrylamide gels under reducing conditions. After SDS-PAGE, proteins were transferred to nitrocellulose membranes. The membranes were blocked with 5% non-fat dry milk (Bio-Rad Laboratories, Inc., Richmond, CA) and incubated with the specific antibody. After three washes, filters were incubated for 1 h at room temperature with horseradish peroxidase-conjugated secondary antibody (Bio-Rad). The membranes were then stained using a chemiluminescence system (ECL-Amersham Biosciences) and then exposed to X-ray film (Kodak). Immunoreactive bands were quantified using Quantity One 1-D analysis software (Bio-Rad).

Capillary-like tube formation assay

A 24-well plate was coated with 230 μl/well Matrigel 13 mg/ml for 30 min at 37°C. PAE cells (8 × 10⁴ cells/ml) were seeded in 500 μl of Ham's-F12 medium in the presence of Met-F-AEA at the final concentration of 10 μM plus bFGF (10 ng/ml). Complete Ham's-F12 medium plus bFGF and not supplemented Ham's-F12 basal medium were used as positive and negative controls, respectively. After 6 h of incubation, capillary-like tube formation was examined under an inverted phase microscope. Cells were fixed with PBS containing 0.2% glutaraldehyde, 1% paraformaldehyde, photographed, and analyzed by Scion Image software.

Gelatin zymography

Quiescent HUVECs were serum-starved, pre-treated with Met-F-AEA (10 μM, 30 min), and then stimulated with bFGF (10 ng/ml) for 24 h. The conditioned media were collected and clarified by centrifugation. Conditioned media containing equal amounts of secreted proteins were mixed with non-reducing Laemmli sample buffer (2×) and subjected to 7.5% SDS-polyacrylamide gels containing 1 mg/ml gelatine (Sigma). The gels were then incubated for 30 min at room temperature twice in 2.5% (v/v) Triton X-100 and rinsed five times in distilled water. The gels were incubated at 37°C for a further 18 h in developing buffer (200 mM NaCl, 5 mM CaCl₂, 50 mM Tris/HCl pH 7.6), then stained with 0.1% Coomassie Brilliant Blue R-250 (Bio-Rad), followed by destaining in 10% (v/v) acetic acid/30% (v/v) methanol. Gelatinolytic activity of MMP-2 was detected as unstained bands on a blue background. HUVEC stimulated with PMA (phorbol myristate acetate) (0.1 μM, 24 h) were used as positive control for MMP-2 activity.

Scaffold fabrication

Collagen gels were prepared following manufacturer's procedures. Briefly, 8 ml of collagen were mixed with 1 ml of $10\times$ DMEM and 1 ml of 0.1 M NaOH solution.

The semi-interpenetrated networks of collagen-hyaluronic acid (CHA SIPNs) were obtained by promoting collagen fibrillogenesis in the presence of HA, following a previously reported protocol (Xin et al., 2004). The resulting solutions have a final HA concentration 5 mg/ml and a collagen final concentration of 1.2 mg/ml. Fibrillogenesis of collagen was induced by incubating the solutions at 37°C for about 45 min, until a firm hydrated gel was obtained.

Fluorescent cell labeling

The PAE cells were labeled using the Cell tracker Green CMFDA (5-chloromethylfluorescein diacetate, Molecular Probes, Invitrogen, Milan, Italy). A subconfluent monolayer of PAE was washed once with PBS $1\times$, labeled with CMFDA $10\ \mu\text{M}$ for 30 min at 37°C , and then washed and incubated for at least 30 min in complete culture medium before trypsinization. Following the same protocol, KiMol were labeled using the Cell tracker orange CMTMR ((5-(and-6-)-(((4-chloromethyl)benzoyl)amino)tetramethylrhodamine), Molecular Probes). Quality of cell labeling was examined using confocal microscope Zeiss LSM 510, equipped with an argon laser at a wavelength of 488 nm for FITC or with a HeNe laser at a wavelength of 543 nm for TRITC. The emitted fluorescence was detected using filters LP 505 and HFT 488 for FITC and using filters LP 560 and HFT 488/543 for TRITC. Images were acquired with an objective of $10\times$ at a resolution of 512×512 or $1,024\times 1,024$ pixel.

Generation of endothelial and tumor spheroids

Endothelial cell spheroids were generated as described elsewhere (Korff and Augustin, 1998). Briefly, confluent monolayers of pre-stained PAE cells were trypsinized. Cells (700 cells per spheroid) were suspended in culture medium containing 0.25% (w/v) carboxymethylcellulose (Sigma), and seeded into non-adherent round-bottom 96-well plates. Under these conditions, all suspended cells contribute to the formation of a single endothelial cell spheroid. These spheroids were harvested within 24 h and used for the following experiments. The same protocol was used to form tumor cell (KiMol) spheroids.

In vitro sprouting angiogenesis assay-three-dimensional spheroids co-cultures

The two different cell spheroids populations (PAE and KiMol spheroids) were harvested and then used for mono- and co-culture experiments. Cellular spheroids were isolated and suspended in a solution of bovine origin type I collagen (1.2 mg/ml) and in collagen type I (1.2 mg/ml)-HA (5 mg/ml) in Ham's F12 medium supplemented with 5% FBS. Then, the spheroids suspension was pipetted into Petri dish for suspension culture and warmed to 37°C for 30 min to allow polymerization of the collagen; a 1.2 mg/ml basement collagen gel layer cell-free was stratified before adding the suspension culture, to avoid spheroids attachment on the bottom of the plate. After polymerization, warmed serum-free Ham's-F12 medium was added to the plates and changed every 48 h.

A total of 12 spheroids were used for each experiment; co-cultures were composed of 6 spheroids of each cell line. The sprouting angiogenesis in gel, in terms of the cumulative length of all the capillary-like sprouts (CLS) originating from the center of the spheroid, the average length of CLS of the spheroid and the number of CLS per spheroid, was quantified using the digitized imaging system, Image Analysis Software MetaMorph USA, connected to an inverted microscope (IX50 Olympus). The number of sprouts per spheroid of endothelial cells was calculated by measuring the length of the sprouts of each spheroid every 24 h for 3 days.

Chick embryo chorioallantoic membrane assay

Fertilized chicken eggs were incubated under conditions of constant humidity at 37°C . On the 4th day of incubation, a window was opened in the eggs-shell after removal of 3–4 ml of albumen so that the developing CAM was kept detached from the shell. The window was sealed with a piece of adhesive tape and the eggs were incubated at 37°C . On the 9th day Met-F-AEA, pre-encapsulated in 1.5% alginate bead, was applied onto CAM of the eggs. The allantoic vessels around

the cells' pellets were counted under a stereomicroscope and photographed with a digital camera at the time of cell implants and 72 h later.

Statistical analysis

All data were presented as means \pm SE. Statistical analysis was performed using one-way ANOVA. In the case of a significant result in the ANOVA, Student's *t*-test was used for dose-response curve. A *P*-value less to 0.05 was considered statistically significant.

Results

Met-F-AEA inhibits bFGF-induced endothelial cell proliferation in vitro

It has already been reported that HUVECs express functional cannabinoid CBI receptors (Liu et al., 2000). In this study, at first we confirmed, through a Western blot analysis on cell lysates, that PAE cells also, the other angiogenic model used, express CBI receptors. Moreover, we observed that incubation with the CBI agonist Met-F-AEA ($10\ \mu\text{M}$, 24 h) decreases CBI protein expression in both endothelial cell types (Fig. 1A).

In order to evaluate Met-F-AEA effect on endothelial cell proliferation in vitro, its inhibitory potency on bFGF-induced proliferation was evaluated. PAE cells were treated with increasing concentrations of Met-F-AEA for 24 h in the presence of bFGF (10 ng/ml) and DNA synthesis was determined by measuring [^3H]-thymidine incorporation. We found that Met-F-AEA inhibits PAE proliferation in a dose-dependent manner, the effect being statistically significant from 5 to 20 μM concentrations (with a dose-dependency between 5 and 10 μM) and the lowest effective dose was 10 μM (Fig. 1B). Below 5 μM dose, we did not observe a statistically significant anti-proliferative effect. These inhibitory effects were not due to cytotoxicity of Met-F-AEA in endothelial cells since Met-F-AEA had no effect on endothelial cell normal growth without bFGF stimulation (Fig. 1C). Furthermore, to determine the involvement of CBI receptor in the anti-proliferative activity of Met-F-AEA, the effect of the selective CBI antagonist SR141716 on bFGF-induced proliferation was tested. The anti-proliferative effect observed was almost totally counteracted by pre-incubation with SR141716, indicating that inhibition of proliferation depends on CBI receptor signaling (Fig. 1B). Similar data were obtained with both endothelial cell types (data not shown).

Met-F-AEA induces apoptosis in endothelial cells

To further investigate the nature of growth inhibition induced by Met-F-AEA, cell-cycle phase distribution was assessed by flow cytometry. Cell-cycle phase distribution was not altered by Met-F-AEA ($10\ \mu\text{M}$, 24 h) treatment, whereas we observed that Met-F-AEA-induced apoptosis (Fig. 2A, 20% of sub-G1 positive cells compared to the control), confirmed also by a flow cytometric assay with annexinV/propidium iodide double staining (Fig. 2B, parts a,b). It has already been reported that anandamide induces apoptosis in HUVECs via vanilloid receptor VRI stimulation (Yamaji et al., 2003). Therefore, we also investigated the role of CBI receptor signaling pathway in the pro-apoptotic action of Met-F-AEA; pre-treatment with the CBI antagonist SR141716 (0.1 μM , 30 min) before Met-F-AEA exposure partially prevented the induction of apoptosis (Fig. 2B, part c). Comparable results were obtained in both cell types (data not shown).

Met-F-AEA causes downregulation/modulation of signaling molecules

To determine which down-stream signaling pathway was influenced by Met-F-AEA treatment, we first probed the expression and phosphorylation of ERK.

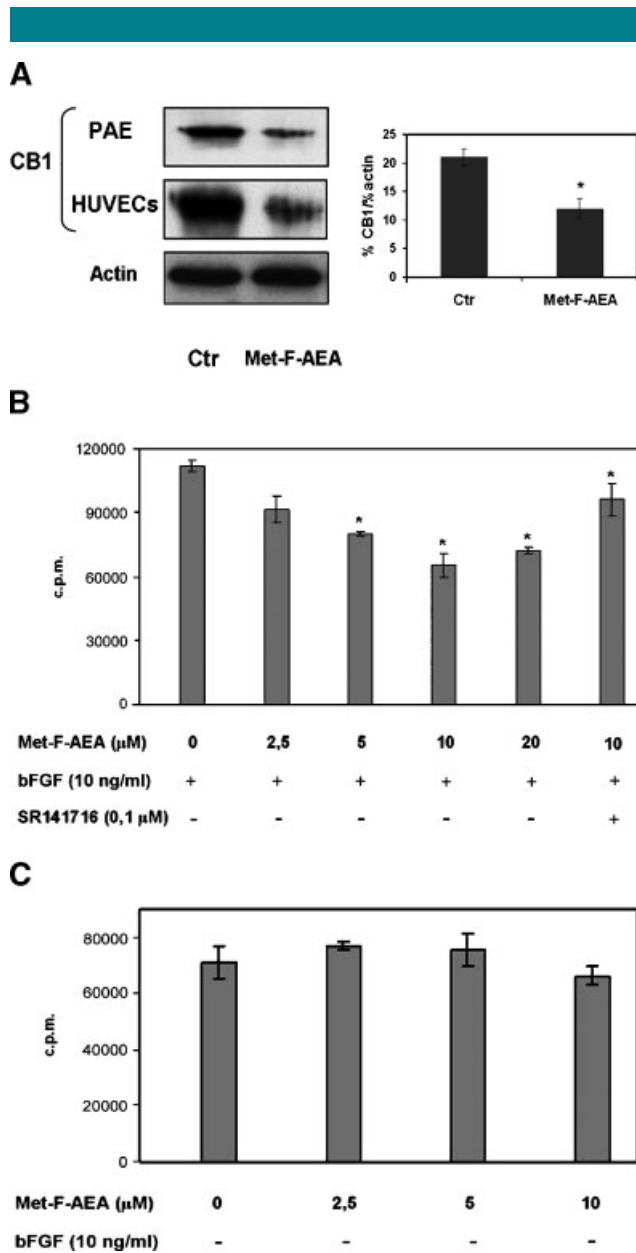


Fig. 1. **A:** Endothelial cells (PAE and HUVECs) express CB1 receptor. Endothelial cells were treated or not with Met-F-AEA (10 μM) for 24 h. After the treatment, cell lysates were blotted with anti-CB1 antibody. Same filters were stripped and re-probed with rabbit polyclonal anti-actin antibody, as loading control. Immunoreactive bands were quantified using Quantity One program. The diagram shows quantification of the intensity of bands, calibrated to the intensity of the actin bands, expressed as means ± SE (* $P < 0.05$ for Met-F-AEA vs. ctr). Each experiment was repeated at least three times. The figure shows a representative blot. **B–C:** Met-F-AEA inhibits bFGF-induced endothelial cell proliferation. PAE cells (3×10^4 /well) were cultured in triplicate for 24 h with concentrations of Met-F-AEA ranging from 2.5 to 20 μM in the presence (B) or not (C) of bFGF (10 ng/ml) or SR141716 (0.1 μM). After 24 h incubation, [3 H]-thymidine incorporation (0.5 μCi/well) was measured. The graphs report the mean ± SE values of three independent experiments. Results were statistically significant (Student's *t* test, Met-F-AEA vs. control, and Met-F-AEA + SR141716 vs. Met-F-AEA, * $P < 0.05$).

Serum-starved HUVECs were pre-treated 30 min with Met-F-AEA followed by the addition of 10 ng/ml bFGF for 15 min. Our results showed that ERK phosphorylation is reduced of 40% by Met-F-AEA treatment and this effect is reversed by CBI antagonist (Fig. 2C).

Among the pathways that control cell survival in endothelial cells, we investigated p38 MAPK and NFκB pathways. In order to investigate if p38 MAPK pathway was involved in the induction of apoptosis, we incubated HUVECs with p38 MAPK inhibitor (10 μM, 1 h) before Met-F-AEA exposure (10 μM, 24 h). We observed that p38 MAPK inhibition partially prevents the trigger of apoptosis by Met-F-AEA, as the CBI antagonist, demonstrating that p38-MAPK-signaling pathway is required for Met-F-AEA-induced apoptotic signals in endothelial cells (Fig. 2B, part d).

Activation of NFκB is considered to play an important role in cell death and apoptosis. To study the effect on NFκB in Met-F-AEA-induced apoptosis in HUVECs, first, Western blot analysis was performed. With increasing time, there was a decrease of non-phosphorylated form of IκBα, targeted for degradation by phosphorylation on Ser 32, which indicated the involvement of NFκB activation following Met-F-AEA treatment in HUVECs (Fig. 3A).

Moreover, when the activity of NFκB was inhibited with synthetic phosphorothioate oligodeoxynucleotides, endothelial cells were not prevented from undergoing apoptosis, rather there was a little increment in the percentage of annexin V⁺ cells (Fig. 3B).

These data indicate that in our model, Met-F-AEA induces apoptosis through CBI receptor signaling and p38 MAPK pathway, whereas a causal relation between NFκB activation and cell death could not be demonstrated, suggesting that the activation of NFκB by Met-F-AEA is not necessary for apoptotic signaling in this system.

Met-F-AEA inhibits capillary-like tube formation on Matrigel

Afterwards, Met-F-AEA was tested for its inhibitory potency on the differentiation of endothelial cells into tube-like structures, another endothelial cell function crucial to angiogenesis. In vitro bi-dimensional tube formation assay was carried out plating PAE cells onto a Matrigel coat. Angiogenic response was measured by the extent and shape of the capillary like network originated in response to Met-F-AEA (10 μM) after 6 h in the presence of bFGF (10 ng/ml) (Fig. 4B). As control (Fig. 4A), the cells were incubated in complete medium normally utilized for their in vitro growth (5% FBS medium) supplemented with bFGF (10 ng/ml). Met-F-AEA seemed to be effective in inhibiting bFGF-induced capillary network formation by significantly reducing the number of tube-like structures' intersections, measured by means of Scion image software, as reported in the histogram (Fig. 4C).

Met-F-AEA effect on secreted MMP-2 activity

Matrix metalloproteinases (MMPs) secreted by endothelial cells are hypothesized to play a key role in the processes of matrix remodeling and endothelial sprouting during angiogenesis (Bussolino et al., 1997; Davis and Senger, 2005). To assess whether Met-F-AEA also interferes with MMP-2 activity in endothelial cells, HUVECs were serum-starved, pre-treated with Met-F-AEA (10 μM, 30 min) alone or in combination with the CBI antagonist SR141716 (0.1 μM), and then stimulated with bFGF (10 ng/ml) for 24 h. HUVECs stimulated with PMA (0.1 μM, 24 h) were used as positive control for MMP-2 (72 kD gelatinase A) activity (Lafleur et al., 2001). The effect on MMP-9 secretion could not be assessed in HUVECs because very low to undetectable levels of MMP-9 are secreted (data not shown). As shown in Figure 4D, treatment with Met-F-AEA for 24 h led to a decrease of MMP-2 gelatinolytic activity as detected by gelatin zymography analysis. The extent of MMP-2 inhibition was significant (* $P < 0.05$). However, when HUVECs were exposed to CBI antagonist SR141716 in combination with

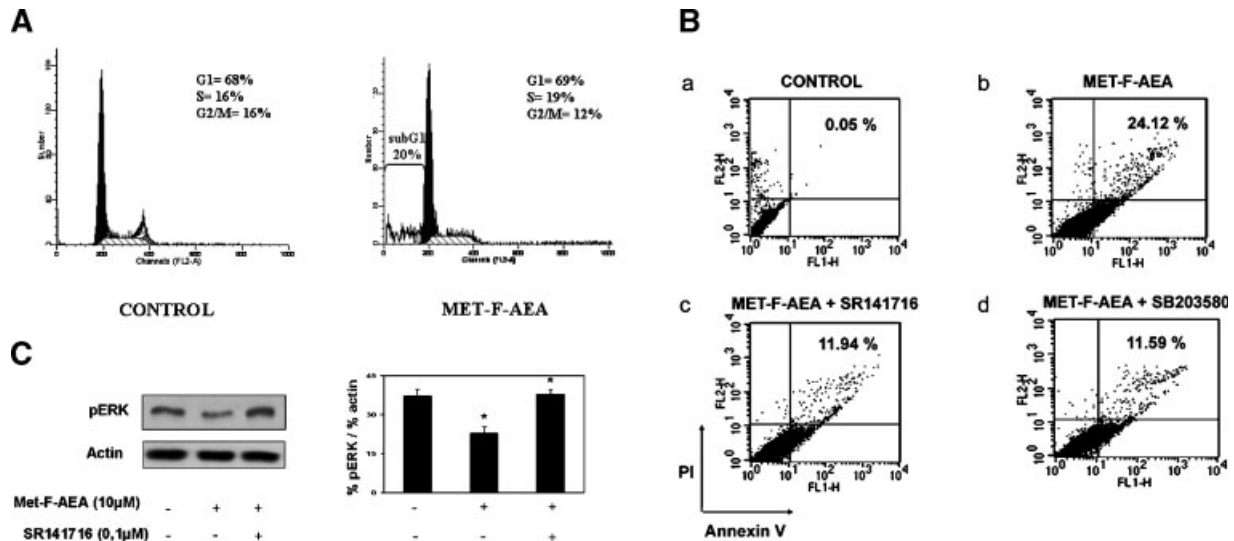


Fig. 2. Effect of Met-F-AEA on apoptosis and cell-cycle progression of endothelial cells. **A:** Endothelial cells treated with Met-F-AEA 10 μ M for 24 h were stained with propidium iodide and analyzed by flow cytometry. Data were subjected to ModFit analysis. Control and Met-F-AEA parts show the relative percentage of cells in the G0/G1, S, and G2/M phases. Apoptosis was calculated as the percentage of cells showing a sub-diploid (sub-G1) DNA peak. The results reported in the histograms are representative of three independent experiments with similar results. **B:** Apoptosis was additionally evaluated by using an annexin V/propidium iodide double staining technique. Endothelial cells were treated with Met-F-AEA 10 μ M for 24 h; then cells were processed and apoptosis was analyzed by flow cytometry as described in Methods. Pre-treatments with CBI antagonist, SR141716 (0.1 μ M, 30 min) or with p38 MAPK inhibitor, SB203580 (10 μ M, 1 h) before Met-F-AEA exposure were also evaluated. In each part is shown the percentage sum of annexin V⁺ and annexin V⁺/propidium iodide⁺ cells. The parts are representative of four independent experiments. **C:** Effect of Met-F-AEA on ERK expression and phosphorylation. Starved HUVECs were pre-treated with Met-F-AEA or with Met-F-AEA + SR141716 for 30 min before incubation with bFGF for 15 min (to induce pERK). After treatment, cell lysates were blotted with anti-pERK antibody. Same filters were stripped and re-probed with rabbit polyclonal anti-total ERK antibody and again with polyclonal anti-actin antibody, as loading control. Immunoreactive bands were quantified using Quantity One program. The diagram shows quantification of the intensity of the bands, calibrated to the intensity of the actin bands, expressed as means \pm SE (^{*}P < 0.05 for Met-F-AEA vs. ctr and for Met-F-AEA + SR141716 vs. Met-F-AEA). Each experiment was repeated at least three times. The figure shows a representative blot.

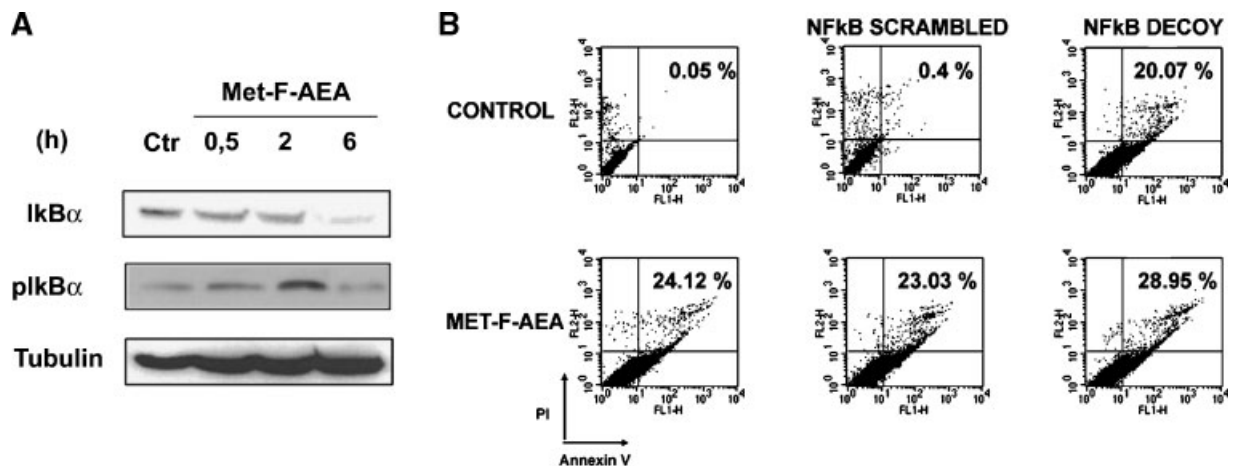


Fig. 3. Effect of Met-F-AEA on NF κ B activation. **A:** HUVECs were treated or not with Met-F-AEA (10 μ M) for various times (from 30 min to 6 h). After treatment, cell lysates were blotted with anti-I κ B α antibody or anti-pI κ B α (Ser32) antibody. Same filters were stripped and re-probed with polyclonal anti-tubulin antibody, as loading control. **B:** Role of NF κ B in Met-F-AEA-induced apoptosis. HUVECs were pre-treated or not with NF κ B synthetic phosphorothioate oligonucleotides (scrambled and decoy, 1 μ M, 1 h) before Met-F-AEA exposure (10 μ M, 24 h); then cells were processed and apoptosis was analyzed by flow cytometry with annexin V/propidium iodide double staining. In each part is shown the percentage sum of annexin V⁺ and annexin V⁺/propidium iodide⁺ cells. The parts are representative of three independent experiments.

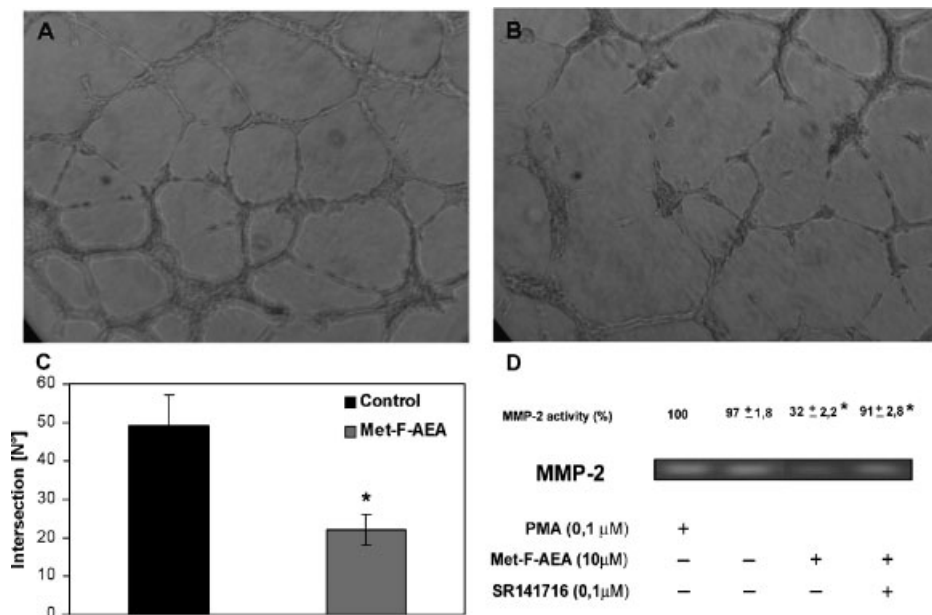


Fig. 4. Met-F-AEA inhibits bFGF-induced PAE capillary-like tube formation after 6 h. **A:** Positive control performed with PAE 5% FBS medium plus bFGF (10 ng/ml), **(B)** conditioned medium (5% FBS medium) containing Met-F-AEA at a concentration of 10 μM plus bFGF (10 ng/ml). Magnification 10×. **C:** Histogram represents the number of intersections calculated by means of Scion Image Software. The number of intersections give a value of the network extension. The graph represents the mean ± SE of the intersections of three independent experiments. Results were statistically significant (ANOVA, * $P < 0.05$). **D:** Effect of Met-F-AEA on secreted MMP-2 activity detected by gelatin zymography. Serum-starved HUVECs were pre-treated with Met-F-AEA (10 μM, 30 min) alone or in combination with SR141716 (0.1 μM) and then stimulated with bFGF (10 ng/ml) for 24 h. The conditioned media were then analyzed by gelatin zymography. HUVECs stimulated with PMA (0.1 μM, 24 h) were used as positive control for MMP-2 activity. The relative pixel density for the 72 kD MMP-2 is shown above. Data of relative pixel density are presented as mean ± SE of four independent experiments of each sample (ANOVA, * $P < 0.05$).

Met-F-AEA, the inhibitory action was prevented, confirming the role of CB1 receptor in the observed effect (Fig. 4D).

Met-F-AEA inhibits angiogenesis in vivo

The anti-angiogenic effect of Met-F-AEA was next studied in vivo chick CAM assays. The inhibitory effects of a representative experiment were depicted in Figure 5. The assay was performed using 1.5% alginate beads incorporating Met-F-AEA at the final concentration of 10 μM (Fig. 5B), as a vehicle for the substance. Empty beads were used as negative control (Fig. 5A). Beads were implanted on the embryonic CAM at day 9 of incubation. After 72 h of implantation, a decrease of vascular reaction was detectable around the beads incorporating Met-F-AEA when compared with the control. Quantitative analysis revealed that Met-F-AEA caused a partial inhibition of angiogenesis in vivo inducing a 2.8-fold reduction in the number of newly formed blood vessels compared with that of vehicle alone (* $P < 0.05$).

Met-F-AEA inhibits tumor-induced angiogenesis in a three-dimensional model in vitro

Finally, the ability of Met-F-AEA to inhibit tumor-induced angiogenesis was examined in vitro using a three-dimensional assay. In brief, PAE cells and KiMol tumor cell spheroids were co-cultured in 3D matrices in order to better mimic the in vivo tumor microenvironment and architecture. We assayed the effect of Met-F-AEA in different 3D scaffolds. In particular, collagen (1.2 mg/ml) and collagen-hyaluronic acid (C 1.2 mg/ml-HA 5 mg/ml) semi-interpenetrating networks (SIPNs) were used in this study. As reported previously (Borselli et al., 2006),

the presence of hyaluronic acid at high dose (5 mg/ml) in collagen gel induced a delay of 24 h of PAE spheroids sprouting angiogenesis. In this study, at first we observed that both tumor spheroids co-cultured or tumor-conditioned medium from KiMol cultures enhanced the angiogenic sprouting of endothelial cell spheroids observed in 3-D polymeric matrices of collagen and collagen-hyaluronic acid (Fig. 6A (parts b,d),B); in particular, the average sprout length ranged from 121 μm in collagen and 10 μm in collagen-hyaluronic (parts a,c) to, respectively, 158 μm and 143 μm in those matrices in presence of either tumor spheroids co-cultured and tumor-conditioned medium from KiMol cultures (parts b,d). Then, in order to verify the inhibitory effect of Met-F-AEA (10 μM) observed in capillary network formation in 2D assays, the spheroids co-cultures were exposed to the substance in three-dimensional polymeric matrices of collagen-hyaluronic acid (Fig. 6C). Met-F-AEA (10 μM), as in 2D assays, seemed to be effective in inhibiting the process of sprouting angiogenesis inducing a strong reduction of both the sprout number (Fig. 6D) and the average sprout length (Fig. 6E).

Discussion

In the present study, we provide direct evidence that Met-F-AEA, a stable analog of the endogenous cannabinoid anandamide, has anti-angiogenic activity in vitro and in vivo that can support its tumor-suppressor action that we previously reported (Bifulco et al., 2001; Portella et al., 2003; Grimaldi et al., 2006).

We found that on the cellular level, Met-F-AEA inhibits bFGF-induced endothelial cell proliferation, tube formation, MMP-2

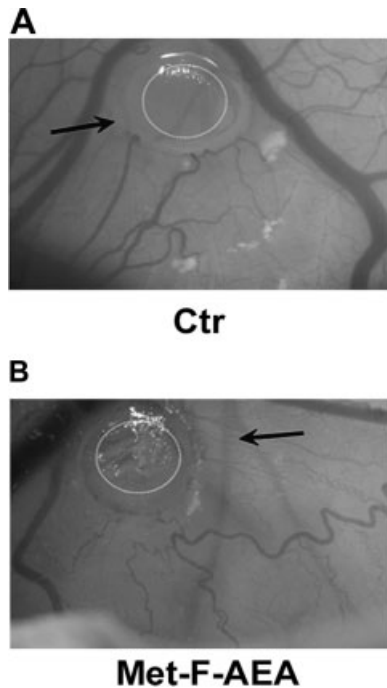


Fig. 5. CAM assay. A: Empty alginate beads. B: Alginate beads incorporating 10 μ M Met-F-AEA. The arrows indicate the alginate beads. The picture is representative of three independent experiments conducted in duplicates.

degrading activity, and induces apoptosis. The lowest effective dose was 10 μ M, the same concentration able to exert anti-proliferative effects also in human breast cancer cells (Grimaldi et al., 2006) and in rat thyroid v-K-*ras*-transformed cells in vitro (Bifulco et al., 2001). Although several cellular parameters are modulated by anandamide already at nanomolar concentrations, such as observed for the vasodilatory action (Wagner et al., 1999), the anti-proliferative effect has been always seen in different cellular models at low micromolar concentrations, up to 20 μ M (Melck et al., 2000; Malfitano et al., 2006). Of note, at higher doses, it has also been reported necrosis in primary hepatic cells (Siegmond et al., 2005). Our study also suggests possible molecular mechanism involved in the anti-angiogenic effect of Met-F-AEA in vitro. Angiogenesis requires coordinated regulation of multiple signaling pathways. Mitogen-activated protein kinases are activated by growth factors, including bFGF and VEGF, and have been implicated to play critical roles during angiogenesis (Beckner, 1999). ERK is usually strongly activated by growth factors and is important for cell proliferation. Our results shows that ERK phosphorylation was reduced of 40% by Met-F-AEA pre-treatment before stimulation with bFGF and this effect was concordant with the inhibition of proliferation. Stress-activated protein kinases, like p38 MAPK, are usually activated by extracellular or intracellular stresses and thus, their activation generally promotes growth inhibition and/or induces apoptosis (Xia et al., 1995). Yue et al. (1999) reported that TLI, a novel TNF α -like cytokine, induced apoptosis in endothelial cells through both JNK and p38 MAPK pathways. Furthermore, it has been previously reported that anandamide, generated by macrophages during shock conditions, induces apoptosis in HUVECs via VRI stimulation triggering phosphorylation of JNK and p38 MAPK (Yamaji et al., 2003). We observed that p38 MAPK inhibition prevents the

induction of apoptosis by Met-F-AEA, demonstrating that p38-MAPK-signaling pathway may play a substantial role in endothelial apoptosis induced by Met-F-AEA.

Another important factor that regulates cell death or survival is the transcription factor NF κ B. In general, NF κ B exists as an inactive form in the cytoplasm, bound to the I κ B inhibitory protein. Various extra-cellular signals induce phosphorylation (at Ser 32 and Ser 36) and subsequent degradation of I κ B, leading to NF κ B activation (Baeuerle and Henkel, 1994; Traenckner et al., 1995). NF κ B has been proposed to function either as a pro-apoptotic or as an anti-apoptotic protein depending on cell type and apoptotic inducers (Beg and Baltimore, 1996; Barkett and Gilmore, 1999). Regarding the relation between NF κ B and CBI receptor agonists/signaling, some studies have suggested that the immunosuppressive function of cannabinoids might be related to the inhibition of NF κ B (Jeon et al., 1996). In another study, the CBI agonist-CP55,940 increased NF κ B activity in PC12 cells also inducing apoptosis, but it was not an integral part of the apoptotic cascade, because its inhibition was not related to the reduction of TUNEL-positive cells (Erlandsson et al., 2002). Do et al. (2004) found a potential link between the THC-induced apoptosis and the activation of NF κ B in dendritic cells. On the contrary, in our study we did not find a causal relation between NF κ B activation and apoptosis induced by Met-F-AEA, indicating that the activation of NF κ B, via activation of the CBI receptor, is not necessary for apoptotic signaling in this system. Maybe only one of the possible homo- or heterodimers of the five members of NF κ B family (p65, Rel B, c-Rel, p50/p105, p52/p100) could be activated by anandamide, and this activation could be liable for the regulation of vascular cell functions not related to apoptosis, such as the expression of vascular cell adhesion molecules (VCAM-1, E-selectin), COX-2, or i-NOS (De Martin et al., 2000). We believe that further studies are required to clarify the meaning of NF κ B activation induced by Met-F-AEA in endothelial cells. In summary, since cannabinoids have been reported to activate c-Jun N-terminal protein kinase and p38 MAPK (Rueda et al., 2000; Derkinderen et al., 2001) and we also observed involvement of p38 MAPK in Met-F-AEA-induced apoptosis, all together these results indicate that activation of CBI by Met-F-AEA in endothelial cells is coupled to multiple signaling pathways; therefore, further investigations are required to understand the causal steps leading to apoptosis.

Previous studies have demonstrated that Met-F-AEA abrogates tumor growth in vitro and in vivo. Met-F-AEA inhibited the growth of a rat thyroid cancer cell-derived tumor in athymic mice by inhibiting the activity of the oncogene product p21 ras and blocked the growth of tumors previously induced in nude mice by the s.c. injection of the same rat thyroid carcinoma cells (Bifulco et al., 2001). Met-F-AEA significantly inhibited, in tumors as well as in transformed cells, the expression of VEGF and its receptor Flt-1/VEGFR-1 (Portella et al., 2003). Furthermore, Met-F-AEA inhibited breast cancer cell proliferation through activation of an S phase checkpoint (Laezza et al., 2006); moreover, it also inhibited adhesion and migration downregulating FAK and Src phosphorylation and significantly reduced the number and dimension of metastatic lung nodules in vivo, via CBI receptor signaling (Grimaldi et al., 2006).

Considering that angiogenesis is essential for tumor growth, progression, and metastasis formation and that tumors can switch on angiogenesis, the anti-tumor effect of Met-F-AEA may be correlated to its anti-angiogenic activity. By using in vitro 2D and 3D models and in vivo CAM assay, we evaluated the anti-angiogenic activities of Met-F-AEA.

Tumors are heterogeneous, with a complex 3D structure; in a tumor mass, the component cell types (tumor cells, endothelial cells, stroma) interact with each other and with their

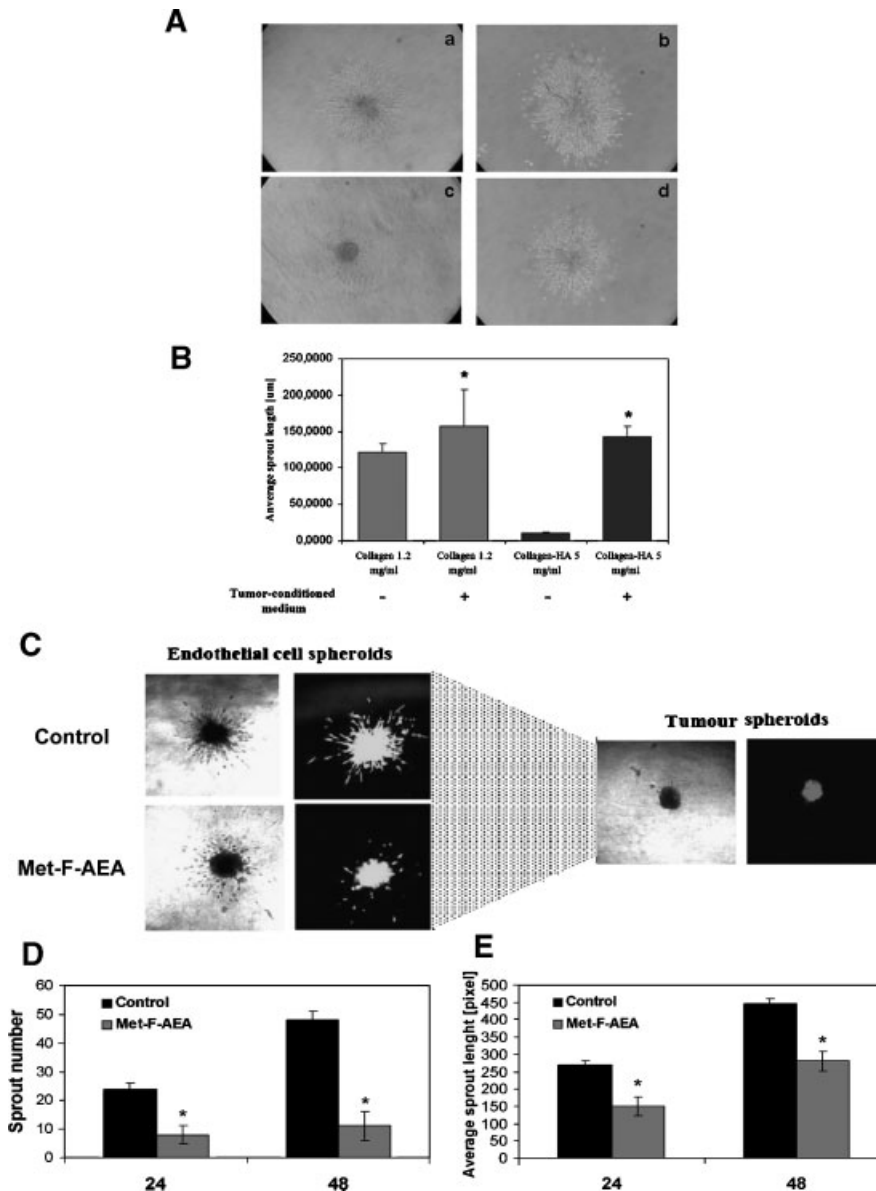


Fig. 6. **A:** PAE spheroids in collagen (a, b) and collagen-hyaluronic acid SIPNs (c, d) in presence of complete medium (a, c) or tumor-conditioned medium from KiMol cultures (b, d). **B:** Quantitative analyses of sprouting. The graph represents the mean \pm SE of the average sprout length of three independent experiments. Results were statistically significant (ANOVA, $*P < 0.05$ for tumor-conditioned medium (+) vs. tumor-conditioned medium (-)). **C:** Light and fluorescent microscopy images of endothelial cell spheroids, without (control) and with Met-F-AEA (10 μ M), and tumor KiMol cell spheroids embedded in three-dimensional collagen-hyaluronic acid SIPNs. **D–E:** Quantitative analyses of sprouting angiogenesis in collagen-hyaluronic acid SIPNs with or without Met-F-AEA. The graphs represent the mean \pm SE of (D) the endothelial sprouts number and (E) the average sprouts length originated by a single endothelial spheroid. Results were statistically significant (ANOVA, $*P < 0.05$).

microenvironment by exchanging information through cell–cell interactions and through interaction with the ECM. The ECM plays a crucial role during angiogenesis; in fact, it provides not only a mechanical support for endothelial cells, but also initiates intracellular signaling through its contact with cell surface proteins (Ingber, 2002). Importantly, MMPs have been shown to play a role in angiogenesis, specifically the gelatinases (MMP-2 and MMP-9), owing to their ability to degrade components of the basement membrane such as type IV collagen and fibronectin, that is a key event in capillary formation (Pepper, 2001). When cultured in a three-dimensional matrix, endothelial cells form tube-like structures, a process that

mimics the steps of capillary formation during angiogenesis. The matrices composed of collagen, fibrin, or hyaluronan represent the major matrix environments where angiogenic or vasculogenic events take place, acting as scaffold proteins for vessel formation (Davis et al., 2002; Yang et al., 2004). Of note, hyaluronan, a core component of ECM is known to contribute to the invasiveness of certain types of cancers (David et al., 2004).

In the present study, the ability of Met-F-AEA to inhibit tumor-induced angiogenesis was examined in vitro using a three-dimensional assay. PAE and KiMol tumor cell spheroids were co-cultured in ECM-like matrices, in order to better mimic the

in vivo tumor microenvironment and architecture. We assayed the effect of Met-F-AEA in different 3D scaffolds (collagen and collagen-hyaluronan). As in 2D models, Met-F-AEA seems to be effective in inhibiting tumor-induced capillary network formation, but in 3D models, needs to be complemented by the action of the specific matrix components. These data underscored the importance of three-dimensional culture condition in order to more closely replicate the in vivo setting and to better characterize anandamide anti-angiogenic activity. In conclusion, the results reported in our present study document the inhibitory actions of an anandamide-derived compound (Met-F-AEA) on several fundamental angiogenic steps, including endothelial cell growth and survival, MMP-2 activity, and in vitro angiogenesis in 2D and 3D models. We also provided some of the potential multiple molecular pathways, downstream of CBI receptor stimulation, involved in the control of endothelial cell functions. It is plausible that the reported anti-angiogenic effects play an important role in mediating the anti-tumor activity of Met-F-AEA in vivo. So our results open the way to further investigations to assess and define the role of the endocannabinoid system in the angiogenic process and the therapeutic potential linked to its pharmacological modulation.

Acknowledgments

This study was supported by Sanofi-Aventis (grant to M.B.) and the Associazione Educazione e Ricerca Medica Salernitana (ERMES). We express our thanks to Dr. Claudio Mauro for the NF κ B Western blot analysis and to Dr. Claudia Grimaldi, Dr. Anna Maria Malfitano, and Dr. Antonietta Santoro for helpful discussion and critical reading of the manuscript.

Literature Cited

- Bauerle PA, Henkel T. 1994. Function and activation of NF κ B in the immune system. *Annu Rev Immunol* 12:141.
- Barkett M, Gilmore TD. 1999. Control of apoptosis by Rel/NF κ B transcription factors. *Oncogene* 18:6910.
- Beckner ME. 1999. Factors promoting tumor angiogenesis. *Cancer Invest* 17:594–623.
- Beg AA, Baltimore D. 1996. An essential role for NF κ B in preventing TNF- α induced cell death. *Science* 274:782.
- Bifulco M, Di Marzo V. 2002. The endocannabinoid system as a target for the development of new drugs for cancer therapy. *Nat Med* 8:547–550.
- Bifulco M, Laezza C, Portella G, Vitale M, Orlando P, De Petrocellis L, Di Marzo V. 2001. Control by the endogenous cannabinoid system of ras oncogene-dependent tumor growth. *FASEB J* 15:2745–2747.
- Bifulco M, Laezza C, Pisanti S, Gazerro P. 2006. Cannabinoids and cancer: Pros and cons of an antitumor strategy. *Br J Pharmacol* 148:123–135.
- Blazquez C, Casanova ML, Planas A, Del Pulgar TG, Villanueva C, Fernandez-Acenero MJ, Aragones J, Huffman JW, Jorcano JL, Guzman M. 2003. Inhibition of tumor angiogenesis by cannabinoids. *FASEB J* 17:529–531.
- Borselli C, Oliviero O, Battista S, Ambrosio L, Netti PN. 2006. Induction of directional sprouting angiogenesis by matrix gradients. *J Biomed Mater Res A* (In press).
- Bussolino F, Mantovani A, Persico G. 1997. Molecular mechanisms of blood vessel formation. *Trends Biochem Sci* 22:251–256.
- Carmeliet P. 2003. Angiogenesis in health and disease. *Nature Med* 9:653–660.
- Casanova ML, Blazquez C, Martinez-Palacio J, Villanueva C, Fernandez-Acenero MJ, Huffman JW, Jorcano JL, Guzman M. 2003. Inhibition of skin tumor growth and angiogenesis in vivo by activation of cannabinoid receptors. *J Clin Invest* 111:43–50.
- David L, Dulong V, Le Cerf D, Chauzy C, Norris V, Delpech B, Lamaz M, Vannier JP. 2004. Reticulated hyaluronan hydrogels: A model for examining cancer cell invasion in 3D. *Matrix Biol* 23:183–193.
- Davis GE, Senger DR. 2005. Endothelial extracellular matrix: Biosynthesis, remodeling, and functions during vascular morphogenesis and neovessel stabilization. *Circ Res* 97:1093–1107.
- Davis GE, Bayless KJ, Mavila A. 2002. Molecular basis of endothelial cell morphogenesis in three-dimensional extracellular matrices. *Anat Rec* 268:252–275.
- De Martin R, Hoeth M, Hofer-Warbinek R, Schmid JA. 2000. The transcription factor NF- κ B and the regulation of vascular cell function. *Arterioscler Thromb Vasc Biol* 20:E83–E88.
- De Petrocellis L, Cascio MG, Di Marzo V. 2004. The endocannabinoid system: A general view and latest additions. *Br J Pharmacol* 141:765–774.
- Derkinderen P, Ledent C, Parmentier M, Girault JA. 2001. Cannabinoids activate p38 mitogen-activated protein kinase through CBI receptors in hippocampus. *J Neurochem* 77:957.
- Do Y, McCallip RJ, Nagarkatti M, Nagarkatti PS. 2004. Activation through cannabinoid receptors 1 and 2 on dendritic cells triggers NF κ B-dependent apoptosis: Novel role for endogenous and exogenous cannabinoids in immunoregulation. *J Immunol* 173:2373–2382.
- Erlanson N, Baumann OG, Rossler K, Kaufmann KM, Giehl T, Wirth T, Thiel G. 2002. Lack of correlation between NF κ B activation and induction of programmed cell death in PC12 pheochromocytoma cells treated with 6-hydroxydopamine or the cannabinoid receptor 1-agonist CP55,940. *Biochem Pharmacol* 64:487.
- Ferrara N, Kerbel RS. 2005. Angiogenesis as a therapeutic target. *Nature* 438:967–974.
- Folkman J. 1995. Angiogenesis in cancer, vascular, rheumatoid and other disease. *Nat Med* 1:27–31.
- Grimaldi C, Pisanti S, Laezza C, Malfitano AM, Santoro A, Vitale M, Caruso MG, Notarnicola M, Iacuzzo I, Portella G, Di Marzo V, Bifulco M. 2006. Anandamide inhibits adhesion and migration of breast cancer cells. *Exp Cell Res* 312:363–373.
- Guzman M. 2003. Cannabinoids: Potential anticancer agents. *Nat Rev Cancer* 3:745–755.
- Hisano N, Yatomi Y, Satoh K, Akimoto S, Mitsumata M, Fujino MA, Ozaki Y. 1999. Induction and suppression of endothelial cell apoptosis by sphingolipids: A possible in vitro model for cell-cell interactions between platelets and endothelial cells. *Blood* 93:4293–4299.
- Ingber DE. 2002. Mechanical signalling and the cellular response to extracellular matrix in angiogenesis and cardiovascular physiology. *Circ Res* 91:877–887.
- Jeon YJ, Yang JT, Pulaski T, Kaminski NE. 1996. Attenuation of inducible nitric oxide synthase gene expression by Δ^9 -tetrahydrocannabinol is mediated through the inhibition of NF κ B/Rel activation. *Mol Pharmacol* 50:334.
- Korff T, Augustin HG. 1998. Integration of endothelial cells in multicellular spheroids prevents apoptosis and induces differentiation. *J Cell Biol* 143:1341–1352.
- Laezza C, Pisanti S, Crescenzi E, Bifulco M. 2006. Anandamide inhibits Cdk2 and activates Chk1 leading to cell cycle arrest in human breast cancer cells. *FEBS Lett* 580:6076–6082.
- Lafleur MA, Hollenberg MD, Atkinson SJ, Knauper V, Murphy G, Edwards DR. 2001. Activation of pro-matrix metalloproteinase-2 (pro-MMP-2) by thrombin is membrane-type-MMP-dependent in human umbilical vein endothelial cells and generates a distinct 63 kDa active species. *Biochem J* 357:107–115.
- Liu J, Gao B, Mirshahi F, Sanyal AJ, Khanolkar AD, Makriyannis A, Kunos G. 2000. Functional CBI cannabinoid receptors in human vascular endothelial cells. *Biochem J* 346:835–840.
- Malfitano AM, Matarese G, Pisanti S, Grimaldi C, Laezza C, Bisogno T, Di Marzo V, Lechler RI, Bifulco M. 2006. Arvanil inhibits T lymphocyte activation and ameliorates autoimmune encephalomyelitis. *J Neuroimmunol* 171:110–119.
- Melck D, De Petrocellis L, Orlando P, Bisogno T, Laezza C, Bifulco M, Di Marzo V. 2000. Suppression of nerve growth factor Trk receptors and prolactin receptors by endocannabinoids leads to inhibition of human breast and prostate cancer cell proliferation. *Endocrinology* 141:118–126.
- Pepper MS. 2001. Role of the matrix metalloproteinase and plasminogen activator-plasmin systems in angiogenesis. *Arterioscler Thromb Vasc Biol* 21:1104–1117.
- Portella G, Laezza C, Laccetti P, De Petrocellis L, Di Marzo V, Bifulco M. 2003. Inhibitory effects of cannabinoid CBI receptor stimulation on tumor growth and metastatic spreading: Actions on signals involved in angiogenesis and metastasis. *FASEB J* 17:1771–1773.
- Risau W. 1997. Mechanisms of angiogenesis. *Nature* 386:671–674.
- Romano MF, Lamberti A, Tassone P, Alfinito F, Costantini S, Chiurazzi F, DeFrance T, Monelli P, Tuccillo F, Turco MC, Venuta S. 1998. Triggering of CD40 antigen inhibits fludarabine-induced apoptosis in B chronic lymphocytic leucemia cells. *Blood* 92:990–995.
- Rueda D, Galve-Roperch I, Haro A, Guzman M. 2000. The CBI cannabinoid receptor is coupled to the activation of c-Jun N-terminal kinase. *Mol Pharmacol* 58:814–820.
- Siegmund SV, Uchinami H, Osawa Y, Brenner DA, Schwabe RF. 2005. Anandamide induces necrosis in primary hepatic stellate cells. *Hepatology* 41:1085–1095.
- Traenckner EB, Pahl HL, Henkel T, Schmidt KN, Wilk S, Bauerle PA. 1995. Phosphorylation of human I kappa B-alpha on serines 32 and 36 controls I kappa B-alpha proteolysis and NF-kappa B activation in response to diverse stimuli. *EMBO J* 14:2876–2883.
- Wagner JA, Varga K, Jarai Z, Kunos G. 1999. Mesenteric vasodilation mediated by endothelial anandamide receptors. *Hypertension* 33:429–434.
- Xia Z, Dickens M, Raingeaud J, Davis RJ, Greenberg ME. 1995. Opposing effects of ERK and JNK-p38 MAP kinases on apoptosis. *Science* 270:1326–1331.
- Xin X, Borzacchiello A, Netti PA, Ambrosio L, Nicolais L. 2004. Hyaluronic-acid-based semi-interpenetrating materials. *J Biomater Sci Polym Ed* 15:1223–1236.
- Yamaji K, Sarker KP, Kawahara K, Iino S, Yamakuchi M, Abejama K, Hashiguchi T, Maruyama I. 2003. Anandamide induces apoptosis in human endothelial cells: Its regulation system and clinical implications. *Thromb Haemost* 89:875–884.
- Yang B, Cao DJ, Sainz I, Colman RW, Guo Y. 2004. Different roles of ERK and p38 MAP kinases during tube formation from endothelial cells cultured in 3-dimensional collagen matrices. *J Cell Physiol* 200:360–369.
- Yue TL, Nijl, Romani AM, Gu JL, Keller P, Wang C, Kumar S, Yu GL, Hart TK, Wang X, Xia Z, DeWolf WE Jr, Feuerstein GZ. 1999. TL1 a novel tumor necrosis factor-like cytokine, induces apoptosis in endothelial cells. Involvement of activation of stress protein kinases (stress-activated protein kinase and p38 mitogen-activated protein kinase) and caspase-3-like protease. *J Biol Chem* 274:1479–1486.